



*LIGO Laboratory / LIGO Scientific Collaboration*

LIGO- T040201-00-R

*ADVANCED LIGO*

10/11/2004

---

Detailed Report on Thermal Compensation Effects in  
Advanced LIGO

---

Phil Willems

Distribution of this document:  
LIGO Science Collaboration

This is an internal working note  
of the LIGO Project.

**California Institute of Technology**  
**LIGO Project – MS 18-34**  
**1200 E. California Blvd.**  
**Pasadena, CA 91125**  
Phone (626) 395-2129  
Fax (626) 304-9834  
E-mail: [info@ligo.caltech.edu](mailto:info@ligo.caltech.edu)

**Massachusetts Institute of Technology**  
**LIGO Project – NW17-161**  
**175 Albany St**  
**Cambridge, MA 02139**  
Phone (617) 253-4824  
Fax (617) 253-7014  
E-mail: [info@ligo.mit.edu](mailto:info@ligo.mit.edu)

**LIGO Hanford Observatory**  
**P.O. Box 1970**  
**Mail Stop S9-02**  
**Richland WA 99352**  
Phone 509-372-8106  
Fax 509-372-8137

**LIGO Livingston Observatory**  
**P.O. Box 940**  
**Livingston, LA 70754**  
Phone 225-686-3100  
Fax 225-686-7189

<http://www.ligo.caltech.edu/>

This report attempts to document the analyses of the effects of thermal lensing in Advanced LIGO clearly enough that the methods of calculation, underlying assumptions, and resulting conclusions can be easily checked.

## 1 Assumptions

The only reoptimization of the interferometer assumed between the two candidate substrates is in the size of the test mass. The dimensions are:

**Table 1: substrate dimensions**

	Diameter	Thickness
Sapphire	31.4 cm	13 cm
Fused silica	34 cm	20 cm

The wedges in the optics are at present unknown and not modeled. They are not expected to play a significant role. The material properties of sapphire and fused silica are:

**Table 2: substrate material properties**

	Sapphire	Fused silica
Density $\rho$	3970 kg/m <sup>3</sup>	2202 kg/m <sup>3</sup>
Refractive index $n$	1.7	1.4497
Thermorefractivity (dn/dT)	7.2x10 <sup>-6</sup> /K	8.7x10 <sup>-6</sup> /K
Thermal conductivity $\kappa$	38 W/m/K	1.37 W/m/K
Heat capacity $C$	770 J/kg/K	739 J/kg/K
Thermal Expansion $\alpha$	5.6x10 <sup>-6</sup> /K	5.5x10 <sup>-7</sup> /K

These numbers come from a variety of sources, including Ryan Lawrence's thesis, and in all cases are within 10% of his values. Sapphire has been treated as isotropic in my analyses. The full anisotropy will be modelled in the future, but since sapphire already has inhomogeneous absorption in most of the models this anisotropy is not expected to create a significant change. The elasto-optic effect is also not yet included in these models. Its absence is expected to create a 10% error in the sapphire results and a 1% error in the fused silica results (the HR surface radii of curvature changes, a purely thermoelastic effect, will not have this error).

Much depends upon the absorption in the mirrors, and a variety of different absorption types were considered. The baseline coating absorption is .5 ppm for both substrates. The bulk absorption for fused silica was 2 ppm/cm, which was the larger of the two values Garilynn Billingsley provided. Since coating absorption dominates in fused silica for this bulk absorption the lower value was not

considered. The baseline sapphire absorption was chosen to be 30 ppm/cm, based on what seemed representative of available samples. More typically the actual, very inhomogeneous absorption of the clear Pathfinder sapphire was used. In the central region its absorption too was about 30 ppm/cm. Inhomogeneous coating absorption is a special case, dealt with below.

The light power in the interferometer was set to 850kW in the arms and 2.1kW in the ITM substrates (this includes the double-pass in the substrate). The beam waist was nominally 6 cm, and the test mass HR radius of curvature was 2076 m. Thus the coating absorbs .425W at full interferometer power.

We will treat thermal compensator noise inside the arm cavity as a SUS technical displacement noise source, which in the SUS DRD is required to be less than about

$5 \times 10^{-21}$  m/ $\sqrt{\text{Hz}}$  at 10 Hz, falling roughly as  $(1/f)$  through the GW sensitivity band, although below about 20 Hz the limit is instead  $10^{-20}$  m/ $\sqrt{\text{Hz}}$ , falling as  $(1/f)^2$ .<sup>1</sup> These two frequency regimes are called out separately because different TCS noise couplings match one or the other spectrum. Thermal compensator noise appearing solely in the recycling cavity (as on a compensator plate) has comparable consequence to power- or signal-recycling mirror noise and is assumed to be required to be below the recycling mirror requirements, which are about  $4 \times 10^{-16}$  m/ $\sqrt{\text{Hz}}$  at 10 Hz, falling to  $10^{-17}$  m/ $\sqrt{\text{Hz}}$  at 100 Hz.<sup>2</sup>

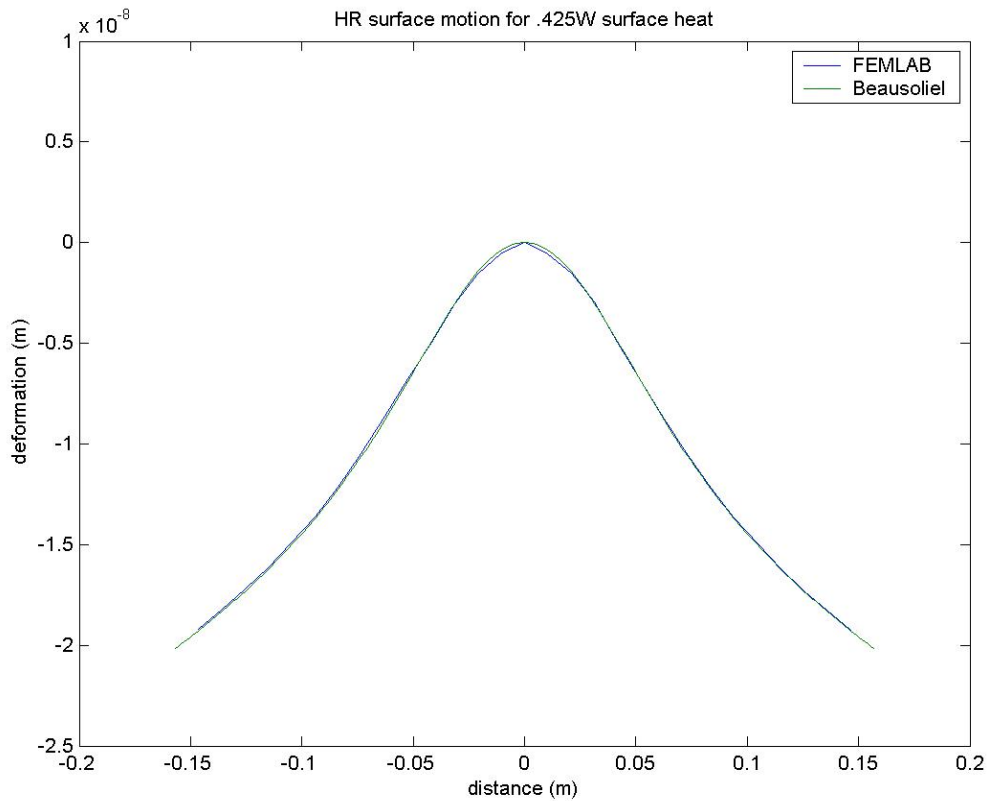
We assume that we can compensate homogeneous and inhomogeneous absorption to the levels demonstrated experimentally by Ryan Lawrence: expressed as a reduction in the power lost from the TEM00 mode on passing through the lens, a factor of 68 reduction of homogeneous absorption and a factor of 8.5 reduction of inhomogeneous absorption. Research may improve our ability to compensate.

## 2 Radius of Curvature Errors

Simplest to analyze are changes in the HR radius of curvature. The interferometer beam heats the middle of the optic, which swells, making the optic flatter and the mode smaller. Compensation can only be done on the test masses themselves, unless compensator plates are put into the arms, an option we exclude here.

Figure 1 shows the expected HR surface deformation for a sapphire ETM at full interferometer power.

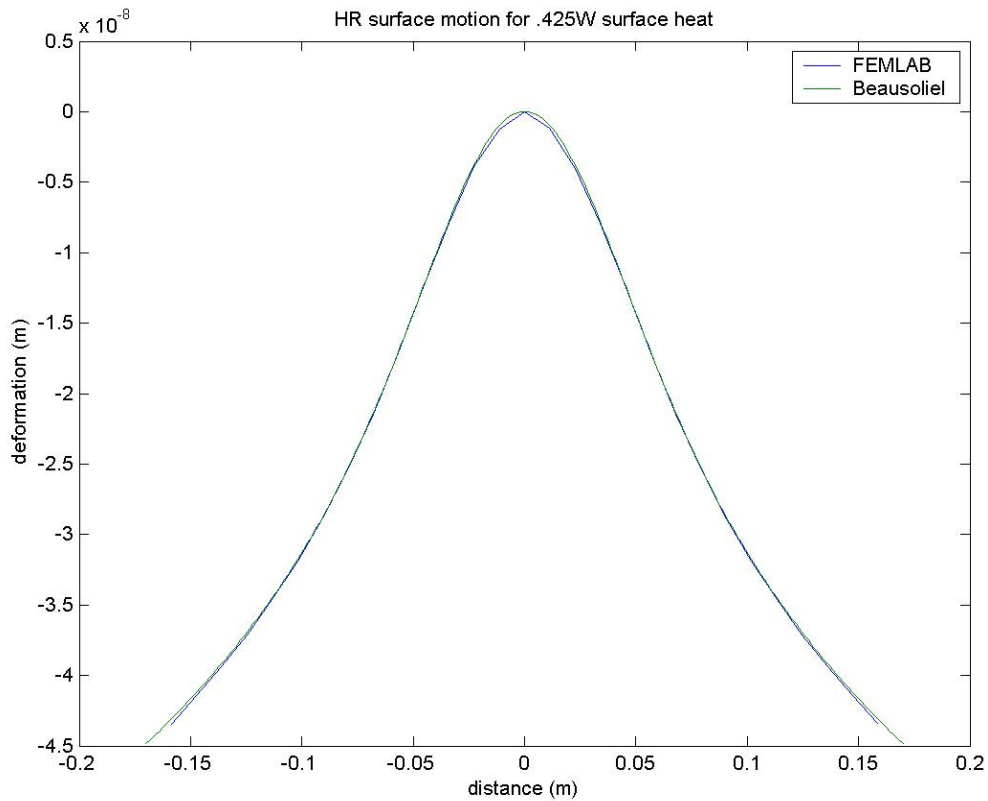
**Figure 1: surface deformation of sapphire ETM**



The two curves are the FEMLAB model and the Hello-Vinet theory as implemented (and corrected) by Ray Beausoliel. Given the existence of a theoretical model for the thermoelastic deformation given uniform absorption of a Gaussian beam, the FEM is not required for this analysis. The comparison is made here to prove the FEM before it is used in the case of inhomogeneous heating later on, where no analytical formula is available.

Figure 2 shows the same analysis for the silica ETM. Note that the size of the effect is about 2 times larger in silica than in sapphire, as is expected from the ratio of  $\alpha/\kappa$  for the two materials.

**Figure 2: surface deformation of silica ETM**



Because compensator noise is expected to be an issue, and because it is easier and more efficient to heat the center of the optic than the rim (thus minimizing temperature rise), we assume here that the interferometer has a point design for correct radius of curvature at full power, and the compensator adds heat to the optic center at lower power.

The thermoelastic analysis was done for sapphire and silica, ETMs and ITMs, and the resulting radii of curvature were estimated by first fitting 8<sup>th</sup> order polynomials to the deformation of a diameter of the HR face and then taking the 2<sup>nd</sup> order coefficient as the inverse of twice the radius of curvature. This gave a value that well approximated the deformation within 6 cm of the optic center. These thermal radii of curvature are listed in Table 3. Finally, we combined these ROCs with the preexisting TM ROCs and calculated the cavity spot sizes. The results are in Table 4. Note that the spot size is not a linear function of the ROC, and so is not a linear function of the laser power.

**Table 3: thermal radii of curvature**

Substrate	Sapphire ETM	Silica ETM	Sapphire ITM	Silica ITM
Thermal ROC	167 km	78.9 km	85.1 km	72.2 km

**Table 4: spot sizes for the two substrates with different levels of compensation**

		ITM spot size	ETM spot size
Silica	Hot, or both compensated	6.0cm	6.0cm
	Cold	8.5cm	8.5cm
	Cold, ITM compensated	6.8cm	6.6cm
Sapphire	Hot, or both compensated	6.0cm	6.0cm
	Cold	7.0cm	7.1cm
	Cold, ITM compensated	6.3cm	6.2cm

### 3 Correction of Radius of Curvature Errors; Noise Couplings

It is worth noting that Ryan Lawrence identified this effect in his thesis. However, he presumed that we would not want to compensate it. This may not be the case. The radius of curvature changes, if uncorrected, will have consequences for interferometer performance: diffraction losses at the optic edge will change, thermal noise will vary with spot size, input coupling efficiency will change with input power. The latter could be corrected with a thermally tunable mode matching telescope. The consequences of not correcting the ROC errors will not be considered further here.

The maximum amount of compensation heat required at the center of optic at low power would ideally be equal to that provided by the interferometer itself at high power, or .425W. In practice, additional compensation may be required to trim engineering tolerance in the point design. We assume 1W compensation power as representative.

The radiation pressure force is just 1W/c, or 3.3nN. Radiation pressure noise falls as  $(1/f)^2$ , so it touches the noise requirements at 10 Hz. The noise force that would produce  $10^{-20}$  m/ $\sqrt{\text{Hz}}$  displacement noise at 10 Hz is  $1.5 \times 10^{-15}$  N/ $\sqrt{\text{Hz}}$ . Thus the RIN of the compensator must be better than  $4.5 \times 10^{-7}$  / $\sqrt{\text{Hz}}$  over the GW band. This is well above the shot noise limit for either 10.6 $\mu\text{m}$  radiation or thermal radiation providing 1W of power.

Thermoelastic noise coupling, as shown in Eq. 2.24 of Ryan Lawrence's thesis, has a  $(1/f)$  dependence:

$$\delta x_{ARM} = \frac{\alpha R(\omega) i}{\rho C \omega} e^{i\omega t} \iint I_c(x, y) \frac{2}{\pi w^2} e^{-2\frac{x^2+y^2}{w^2}} dx dy$$

where R is the fractional ripple on the compensator beam and  $I_c$  is the compensator beam profile. In this case the compensator beam profile is identical to the interferometer beam profile, so the requirement that 1W of compensator power produce less than  $5 \times 10^{-21}$  m/ $\sqrt{\text{Hz}}$  at 10 Hz translates to

a relative intensity noise in the GW band of  $1.0 \times 10^{-8}/\sqrt{\text{Hz}}$  for fused silica and  $1.9 \times 10^{-9}/\sqrt{\text{Hz}}$  for sapphire.<sup>3</sup>

By comparison, the shot noise limit for 1W of CO<sub>2</sub> laser radiation is  $1.4 \times 10^{-10}/\sqrt{\text{Hz}}$ . Compensation without noise is fundamentally possible, though we know of no IR detector with dynamic range at this level. A search for a better way to compensate the radius of curvature errors would be worthwhile. A complementary absorbing coating could be put on the surface to correct the error passively, for example. The best RIN known for an IR sensor is at the  $1 \times 10^{-7}/\sqrt{\text{Hz}}$  level for a cooled HgCdTe detector.

## 4 RF Sideband Buildup in the Recycling Cavities

The RF sidebands are intended only to control the interferometers internal degrees of freedom, and not to heterodyne the gravitational wave sidebands. This makes their mode structure less critical, but also makes harder to quantify the requirements on their mode structure. The current requirement is that the RF sideband power in the recycling cavity not saturate for any power input to the interferometer up to 120W.

In the detuned configuration of Advanced LIGO, there are two pairs of sidebands, each resonating differently in the coupled recycling cavities. There is also the possibility of adjusting the detuning for narrowband operation. Finally, the RF sideband buildup in the presence of thermal aberrations can be complex. To simplify the analysis and get a rough measure of the compensation needs, we assume any RF sideband power scattered out of the fundamental TEM<sub>00</sub> mode to be lost, and model only the power recycling cavity, with a perfectly reflecting back mirror. In this case the power buildup is

$$P_{RF} = \frac{P_{in} R_{RM}}{(1 - \sqrt{T_{RM}}(1 - L))^2}$$

where  $R_{RM}$ ,  $T_{RM}$  are the power recycling mirror reflectivity and transmissivity, and  $L$  is the loss to higher order modes, evaluated by calculating the overlap of the TEM<sub>00</sub> mode with itself after double-passing through the thermal lens. This loss is a quadratic function of the input laser power in the range of input powers we are considering,  $L = (\alpha P_{in})^2$ .

In the case of a homogeneous 30 ppm/cm sapphire, cold curvature optimized, and with no HR surface compensation, we found that  $\alpha = 2.0 \times 10^{-3}/W$ . Figure 3 shows how the RF sideband power will saturate at about 50W input power in the absence of thermal compensation. In his thesis, Ryan Lawrence found this point at about 20W input power using Melody to model an Advanced LIGO without signal recycling. The reason for this discrepancy is not understood. We may easily insert thermal compensation into this model by multiplying  $L$  by a factor between 0 and 1, and we can scale the absorption of sapphire from its nominal 30ppm/cm value by scaling  $\alpha$

by the same factor. Doing this, we find that the RF sideband power buildup just saturates at 120W input if the thermal compensation reduces the loss by a factor of 5.5. Ryan Lawrence was able to demonstrate a factor of 68 reduction in laboratory tests, so 30ppm/cm absorption can be compensated. This factor of 68 reduction becomes just adequate by this standard when the sapphire absorption is increased to 104ppm/cm.

For sapphire, the bulk inhomogeneities are significant. When the uniform 30ppm/cm absorption assumed above for sapphire is replaced by the absorption profile measured for a Pathfinder sapphire, the loss increases from 6% to 11%. Inserting this loss into the formula above (by changing  $\alpha$ ) shows that a factor of 11 loss suppression is necessary to meet the RF sideband power buildup requirement. Ryan Lawrence's proof-of-principle experiment demonstrating inhomogeneous compensation achieved a factor of 8.5 suppression, so the Pathfinder sapphire would not satisfy requirements given currently demonstrated inhomogeneous compensation.

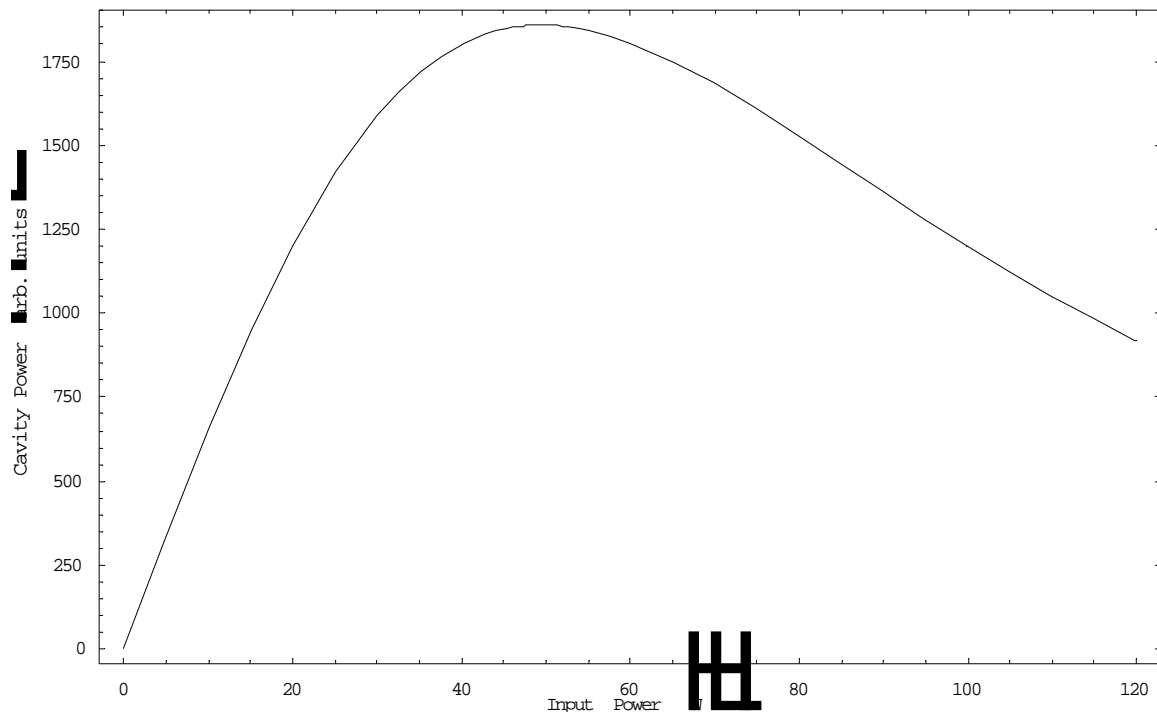


**Figure 3: RF sideband buildup in uncompensated 30 ppm/cm sapphire**

For fused silica, at high power operation the RF sideband optical loss at high power is 93%- the cavity will require a large amount of thermal compensation to build up significant RF sideband power. This degree of compensation should just barely be attainable with a shielded ring heater acting on a compensator plate given the demonstrated performance mentioned above.

These effects would be compensated on a fused silica plate in the recycling cavity. If HR surface compensation were simultaneously applied, the results obtainable would likely be different. This

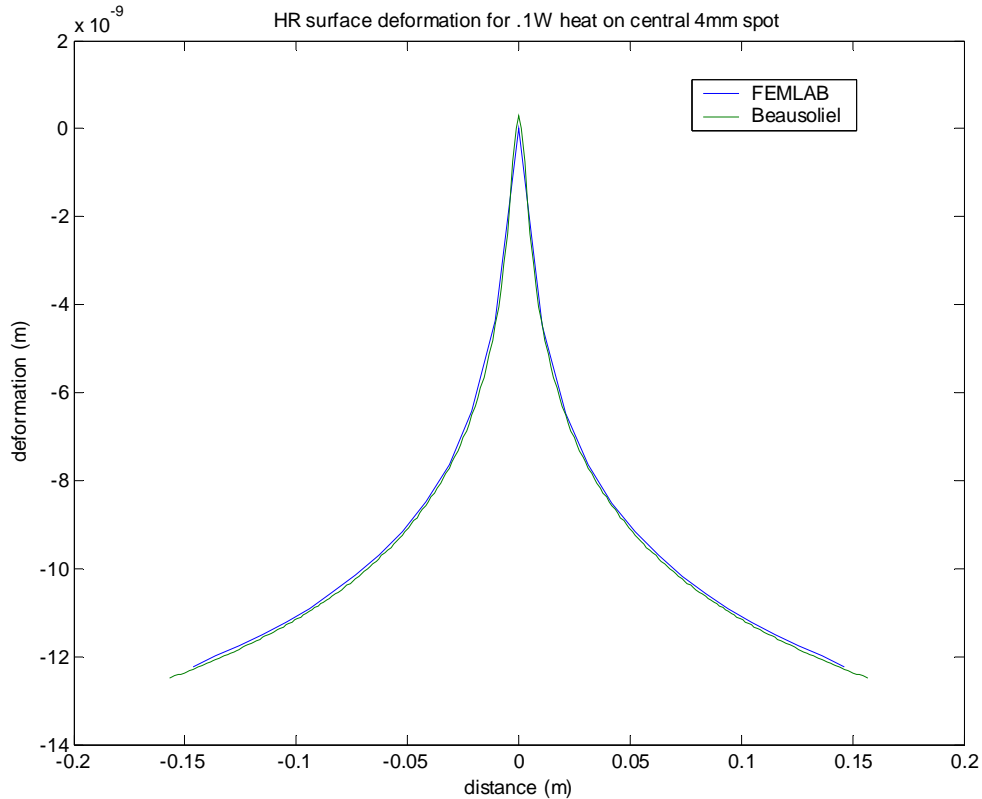
interaction has not yet been studied. All of these analyses deserved to be tested with FFT and Melody.

## 5 Thermal Roughness

Small patches of increased absorption on the HR surfaces of the test masses with heat up and thermally expand, forming ‘blisters’ on the optic surface which will then scatter power from the arm cavity. The scatter loss budget in the arm cavities is very tight- less than 20 ppm per HR surface. This sets limits on the allowable amplitude of features on the HR surface. In previous analyses the thermal deformation from small point absorbers was calculated and the overlap of the TEM00 mode against itself after reflecting from the HR surface was used to estimate the loss. In this document a more detailed analysis that calculates the scatter into all modes that are supported by the arm cavity and excludes them from the loss. These modes are: TEM00, TEM10, TEM01, TEM11, TEM20, TEM02, TEM21, TEM12, TEM30, TEM03. All these modes have diffraction loss at the edges of the sapphire test masses that is less than the ITM transmittance, .005.

Figure 4 shows the surface deformation for centered point coating loss patch.

**Figure 4: surface deformation for a central point absorber on sapphire**



The overlap integral of the arm cavity TEM00 mode with the set of modes listed earlier upon reflection from the thermal roughness shown in Figure 4 gives a .022% loss from the mode for .1 W absorbed.

The power scattered from the arm scales as the square of the deformation amplitude, and thus as the square of the absorbed power:

$$\frac{L_1}{L_2} = \left( \frac{P_1}{P_2} \right)^2$$

Since .1 W absorbed leads to 0.022% scatter, 20 ppm scatter would be caused by 30 mW absorbed power. For 850 kW arm power, the 4 mm spot will need an excess absorption of  $(30\text{mW}/850\text{kW}) \cdot (.06\text{m}/.004\text{m})^2 = 8$  ppm. If the scatter is to be limited to 1 ppm, then the spot absorption must be less than  $8 \text{ ppm}/\sqrt{20}$ , or 1.8 ppm. Spots further from the center can be more absorbing as the incident power there is less and the sensitivity to roughness is lower. Table 5 lays out this variation for sapphire.

**Table 5: power scattered by point absorption in sapphire**

Spot offset from center	Scatter from .1W absorbed	Power needed to scatter 20ppm
0 cm	0.022%	30 mW
2 cm	0.021%	31 mW
4 cm	0.013%	39 mW
6 cm	0.005%	63 mW

For fused silica, .1 W absorbed at the central point causes .15% loss, and 20 ppm scatter would be the result of 12 mW excess power absorbed by the spot, which would thus have an excess absorption of  $(12\text{mW}/850\text{kW}) \cdot (.06\text{m}/.004\text{m})^2 = 3.2$  ppm. If the scatter must be less than 1ppm, then the excess absorption must be less than  $3.2 \text{ ppm}/\sqrt{20}$ , or 0.7 ppm. Table 6 shows the variation of loss with spot location in fused silica.

**Table 6: power scattered by point absorption in silica**

Spot offset from center	Scatter from .1W absorbed	Power needed to scatter 20ppm
0 cm	0.15%	12 mW
2 cm	0.10%	14 mW
4 cm	0.07%	17 mW
6 cm	0.024%	29 mW

The acceptable power absorption in a coating is thus 2x lower for fused silica than sapphire, and fairly stringent.

## 6 Output Coupling Efficiency of Gravitational Wave Sidebands

The effect of thermal lensing on the efficiency of extraction of the gravitational wave sidebands through the signal cavity has been modeled in several ways, all incomplete at some level. Although these different methods roughly agree in their conclusions, detailed modeling with FFT or Melody is essential and is underway.

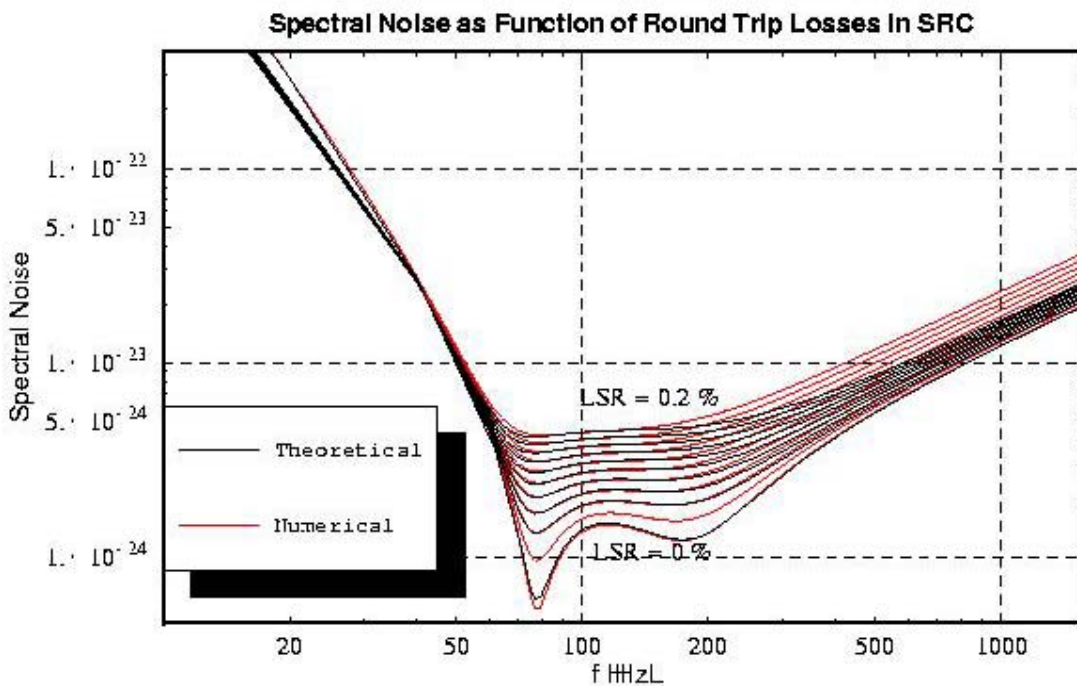
Jim Mason analyzed the transmissivity of signal sidebands through the three mirror cavity in the presence of a loss L in the signal cavity (Eq. 2.32 of his thesis) and found it on resonance to be proportional to a coupling factor

$$t'_{SEC} = \frac{t_{SEM} \sqrt{1-L}}{1-r_{SEM}(1-L)}$$

Using this formula, it is easy to show that the signal transmissivity will drop on resonance by 5% if the loss is about 0.15%.

More recently, Paula Popescu and Tom Corbitt analyzed the interferometer’s full spectral sensitivity using the Buonanno and Chen quantum model. Their results are shown in Figure 5. Like Mason’s analysis, they find that 0.2% loss causes several percent reduction in sensitivity, but only at high frequencies. Since thermal noise is a substantial limit to sensitivity in the important 100 Hz frequency region, and the thermal noise sidebands are also inefficiently coupled through the signal cavity, the effect of these losses on binary inspirals, stochastic sources, and other low frequency sources is relieved. As Figure 6 shows, the loss can be as high as 2% without reducing inspiral range by more than 5%.

**Figure 5: quantum analysis of optical noise in the presence of signal cavity losses. Each curve has 0.2% more loss than the one below it. The numerical curves are expected to be more accurate.**

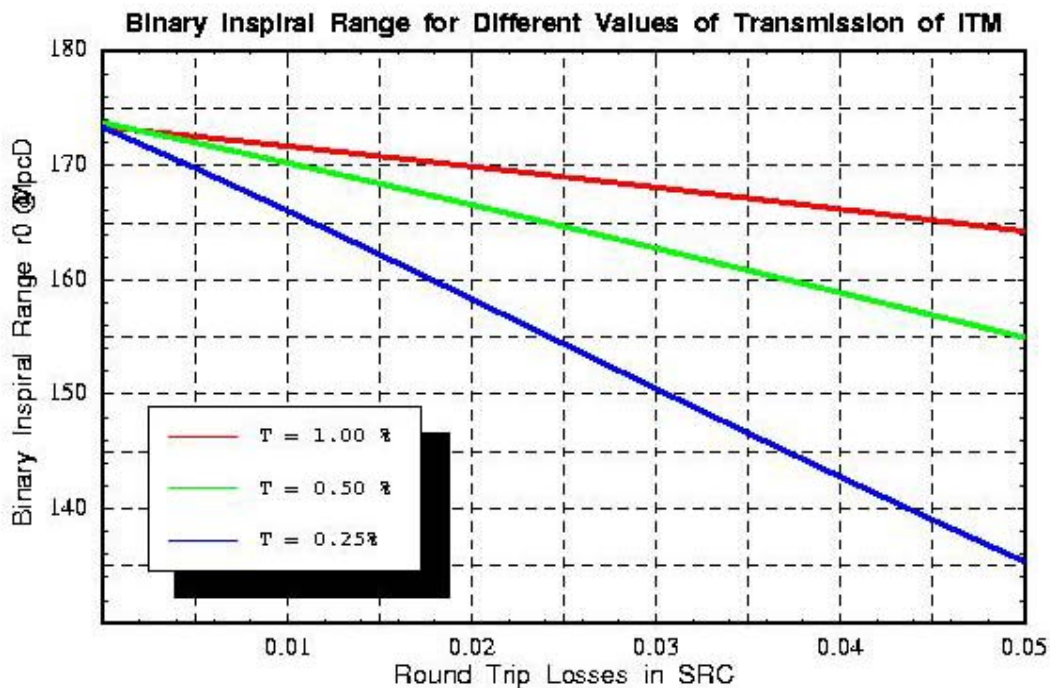


Thermal lensing is not identical to loss, since it upconverts light to higher, possibly resonant modes, rather than simply absorb it. To estimate this effect, we have a Mathematica notebook<sup>4</sup> that

calculates the coupled field equations for two spatial modes resonating in the coupled cavity formed by the arm and signal cavities. These modes are the TEM<sub>00</sub> and TEM<sub>02</sub> modes, and they are coupled by a radius of curvature error (a crude approximation to thermal lensing). This notebook shows a 0.08% effective loss from the TEM<sub>00</sub> mode causing a 5% loss of signal on resonance, as well as peak frequency shifts not observed for pure loss.

These three separate analyses have roughly the same conclusion: that loss at the 0.1% level (whether due to absorption or conversion to higher-order modes, as given by the loss formulae in the RF sideband section) will reduce sensitivity at the 5% level at high frequency.

**Figure 6: inspiral range vs. signal cavity loss**



<sup>1</sup> See LIGO document T-010007-01-D.

<sup>2</sup> See LIGO document T-010097-0-D.

<sup>3</sup> In the latest version of the downselect document (version 7), the noise RIN requirements are two times less strict than this. The difference is that the (1/f) nature of the noise coupling and system requirement was not correctly identified there.

<sup>4</sup> The notebook is “signal extraction calculation for report.nb” and is available for review.